

# Chemical shift anisotropy amplification with high amplification factor and improved sensitivity

Limin Shao<sup>a</sup>, Charles Crockford<sup>b</sup>, Jeremy J. Titman<sup>a,\*</sup>

<sup>a</sup> School of Chemistry, University of Nottingham, University Park, Nottingham, NG7 2RD, UK

<sup>b</sup> School of Physics and Astronomy, University of Nottingham, University Park, Nottingham, NG7 2RD, UK

Received 20 September 2005; revised 13 October 2005

Available online 4 November 2005

## Abstract

An improved version of the recently proposed chemical shift anisotropy amplification experiment is described. The original experiment correlates a fast magic angle spinning spectrum in the  $\omega_2$  dimension with a sideband pattern in  $\omega_1$  in which the intensities mimic those for a sample spinning at a fraction of the rate  $\omega_r/N$ . Advantages of the experiment include the use of standard methods to extract the principal tensor components from the  $\omega_1$  sideband patterns and the small number of  $t_1$  increments required. The improved version described here permits large amplification factors  $N$  to be obtained without resort to prohibitively long sequences of  $\pi$ -pulses and allows sensitivity to be maximized by eliminating the need to store the magnetization along the  $z$ -axis for  $t_1$ . Amplification factors up to 32 are demonstrated experimentally.

© 2005 Elsevier Inc. All rights reserved.

**Keywords:** Chemical shift anisotropy; Magic angle spinning; Spinning sidebands

## 1. Introduction

Recently we introduced a new “chemical shift anisotropy (CSA) amplification” experiment [1–3] which is particularly suitable for measuring small shift tensors. The experiment correlates the standard magic angle spinning (MAS) spectrum in the  $\omega_2$  dimension with a sideband pattern in  $\omega_1$  in which the intensities are identical to those expected for a sample spinning at some fraction  $1/N$  of the actual rate  $\omega_r$ . The sideband pattern in the  $\omega_1$  dimension results from an amplification by a factor  $N$  of the modulation caused by the CSA. A major advantage of the CSA amplification experiment is that long acquisition times can be avoided without loss of resolution of different chemical sites. This is because the isotropic shift appears only in the  $\omega_2$  dimension, and there is no transverse relaxation of the magnetization in the evolution period, so a minimal number of  $t_1$  increments is sufficient.

CSA amplification shares this advantage with recent two-dimensional modifications [4,5] of the PASS technique, originally introduced by Dixon [6]. Dixon’s method employed sequences of variable duration consisting of four  $\pi$ -pulses at timings synchronized with the MAS rotor. These cause a phase shift of magnitude  $M\theta$  for the sideband at a frequency  $M\omega_r$  from the isotropic line, where the angle  $\theta$  is known as the “pitch” of the sequence. In contrast to Dixon’s original experiment, genuine two-dimensional versions of PASS require constant duration sequences with arbitrary pitch. These allow  $\theta$  to be varied over a full period in the evolution dimension, while avoiding differential transverse relaxation between sequences of different duration. In these circumstances, Fourier transform with respect to  $\theta$  results in the separation of different sideband manifolds over the  $\omega_1$  co-ordinate of the two-dimensional spectrum. 2D-PASS was first achieved [4] by setting  $\theta$  proportional to an evolution time  $t_1$ , during which the magnetization is stored along the  $z$ -axis, sandwiched between two sequences of  $\pi$ -pulses with fixed timings. This approach suffers from the drawback that only one

\* Corresponding author. Fax: +44 115 951 3560.

E-mail address: [Jeremy.Titman@nott.ac.uk](mailto:Jeremy.Titman@nott.ac.uk) (J.J. Titman).

component of the magnetization is retained during the evolution time. Hence, two separate experiments are necessary to allow reconstruction of the required two-dimensional FID, resulting in a 2-fold reduction in sensitivity. This problem was later overcome by the discovery of PASS sequences consisting of five  $\pi$ -pulses [5] with constant duration and arbitrary pitch. This approach results in a somewhat unconventional two-dimensional experiment in which the required “ $t_1$  increments” are generated by varying the timings of the  $\pi$ -pulses.

In the original CSA amplification experiment [1,3] the magnetization was stored along the  $z$ -axis during the evolution time. The amplification factor is determined by the fixed timings of the two identical sequences of  $\pi$ -pulses which surround  $t_1$ . This version allowed amplification factors as high as 12 to be realized using up to 14  $\pi$ -pulses in total, but it suffers from the same drawbacks as the first 2D-PASS approach described above. More recently, it has been shown [7] that CSA amplification with  $N$  up to 3 can be achieved by sequences of five  $\pi$ -pulses with variable timings, after the fashion of the second 2D-PASS

approach described above. However, obtaining higher amplification factors using this method requires concatenation of many such sequences, resulting in long durations and large numbers of pulses. For example, an amplification factor of 11 requires 23  $\pi$ -pulses over 16 rotor periods.

In this paper, we describe an alternative CSA amplification experiment which employs the pulse sequence shown in Fig. 1A. Transverse magnetization, generated by cross polarization if appropriate, evolves under a sequence of  $q$   $\pi$ -pulses, before the FID is recorded as a function of  $t_2$ . The timings of the  $\pi$ -pulses are varied to generate  $(q + 1)/2$  FIDs as described below. Double complex Fourier transformation of these produces the required CSA amplification spectrum. In this improved experiment problems associated with storing the magnetization along the  $z$ -axis are eliminated, so that sensitivity is maximized. As will be shown below, the amplification factor increases linearly with the number of  $\pi$ -pulses, according to  $N = q + 1$ . Hence, an added advantage is the ability to realize very high amplification factors without resort to prohibitively large numbers of  $\pi$ -pulses or long sequences.

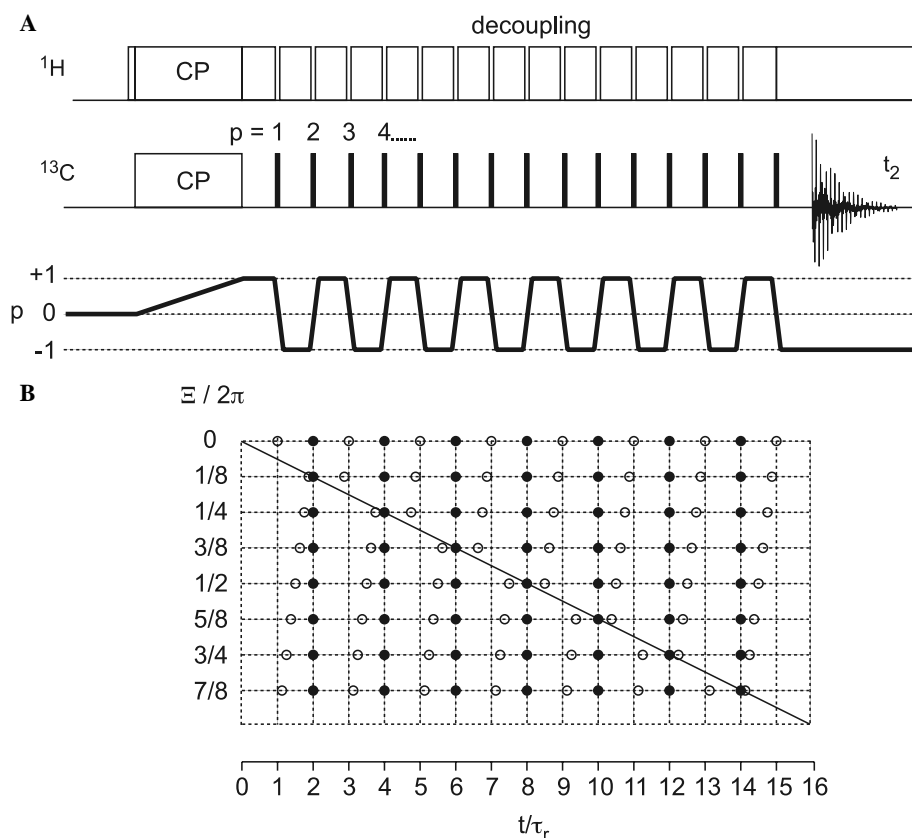


Fig. 1. The pulse sequence used to record improved carbon-13 CSA amplification spectra in this paper. Transverse magnetization, generated by cross polarization if appropriate, evolves under a sequence of  $q$   $\pi$ -pulses, before the FID is recorded as a function of  $t_2$ . The sequence corresponding to  $\Xi = 0$  is shown in (A), in which black rectangles represent carbon-13  $\pi$ -pulses, along with the coherence transfer pathway selected exclusively by a COG31(-16, -15, -16, -15, -16, -15, -16, -15, -16, -15, -16, -15, -16, -15, -16, -15; 0, 0) phase cycle. The timings for the  $\pi$ -pulses in all 8 sequences required for CSA amplification by a factor of 16 are indicated approximately in (B), along with the corresponding values of  $\Xi$ . Unfilled circles show  $\pi$ -pulses which have  $p$  odd, while filled circles represent those with  $p$  even. Accurate values of the timings can be calculated from Eqs. (14) and (15). Note that all 8 sequences result in a spin echo at  $16 \tau_r$ .

## 2. Theory

The orientation of the CSA principal axis system for a given chemical site relative to MAS rotor frame is given by the Euler angles  $(\alpha, \beta, \gamma)$ . Following Antzutkin et al. [8], we consider a “carousel” of sites which have identical values of  $\alpha$  and  $\beta$ , but a uniform and continuous distribution of  $\gamma$  angles. The NMR precession frequency of sites within the carousel  $\omega_c(t; \gamma)$  can be written as a Fourier series

$$\omega_c(t; \gamma) = \sum_{m=-2}^2 \omega_c^{(m)}(\gamma) \exp(im\omega_r t). \quad (1)$$

The coefficients  $\omega_c^{(m)}$  are given by

$$\omega_c^{(m)}(\gamma) = \sum_{n=-2}^2 D_{n-m}^2(\alpha, \beta, \gamma) d_{-m0}^2(\beta_0) A_{2n} + \delta_{m0} \omega_{\text{iso}}, \quad (2)$$

where the  $A_{2n}$  are the components of the CSA tensor,  $\beta_0$  is the magic angle, the isotropic shift  $\omega_{\text{iso}}$  depends on the offset from the carrier frequency  $\omega_{\text{rf}}$

$$\omega_{\text{iso}} = \omega_0(1 - \sigma_{\text{iso}}) - \omega_{\text{rf}} \quad (3)$$

and the Wigner rotations  $D(\alpha, \beta, \gamma)$  and  $d(\beta)$  are defined according to the convention of Spiess [9]. The MAS FID for sites within the carousel  $S_c(t; \gamma)$  can be written as [8]

$$S_c(t; \gamma) = \exp\{i[\omega_c^{(0)} t + \xi_c(t; \gamma) - \xi_c(0; \gamma) + \phi_c(0; \gamma)]\}, \quad (4)$$

where relaxation has been neglected, and  $\xi_c$  is defined by

$$\xi_c(t; \gamma) = \sum_{m \neq 0} \frac{\omega_c^{(m)}(\gamma) \exp(im\omega_r t)}{im\omega_r}. \quad (5)$$

The difference  $\xi_c(t; \gamma) - \xi_c(0; \gamma)$  is the phase angle accumulated by the transverse magnetization during the acquisition time, while  $\phi_c(0; \gamma)$  represents its initial phase which is independent of orientation under normal circumstances. Note that orientations within a carousel experience the same precession frequencies at different time points in a MAS period, resulting in a time/orientation symmetry for  $\xi_c(t; \gamma)$  of the form

$$\xi_c(t; \gamma) = \xi_c(t + \gamma/\omega_r; 0) = \xi_c(0; \gamma + \omega_r t). \quad (6)$$

The two-dimensional FID resulting from a CSA amplification experiment is [1]

$$S_c(t_1, t_2; \gamma) = \exp\{i[N\xi_c(0; \gamma) - N\xi_c(0; \gamma + \omega_r t_1)]\} \\ \times \exp\{i[\omega_c^{(0)} t_2 + \xi_c(0; \gamma + \omega_r t_2) - \xi_c(0; \gamma)]\}. \quad (7)$$

The sideband intensities in the  $\omega_1$  projection of the corresponding spectrum have been shown [3] to be identical to those which would be observed for a sample spinning at  $\omega_r/N$ . In the improved version of CSA amplification described here each “ $t_1$  increment” is generated by a different sequence of  $q$   $\pi$ -pulses. Each sequence prepares the magnetization with a different phase at the start of acquisition

$$\phi_c(0; \gamma) = N\xi_c(0; \gamma) - N\xi_c(0; \gamma + \Xi), \quad (8)$$

where the phase angle  $\Xi$  is a function of the  $\pi$ -pulse timings, but independent of crystallite orientation. It should be noted

that  $\Xi$  plays a similar, but not identical, role to the pitch  $\Theta$  in 2D-PASS. To achieve CSA amplification a set of sequences must be found which allow  $\Xi$  to be incremented between 0 and  $2\pi$ , such that a discrete Fourier transform with respect to  $\Xi$  generates the required  $\omega_1$  spectrum.

The phase accumulated during a sequence of  $q$   $\pi$ -pulses with total duration  $T$  is [8]

$$\phi_c(0; \gamma) = \omega_c^{(0)} \tau + \xi_c(0; \gamma) \\ - (-1)^q \left\{ 2 \sum_{p=1}^q (-1)^p \xi_c(t^{(p)} - T; \gamma) + \xi_c(-T; \gamma) \right\}, \quad (9)$$

where the time origin has been assumed to be at the end of the sequence, the  $\pi$ -pulses are applied at timings  $t^{(p)} - T$  where  $p = 1, 2, \dots, q$  and the rf field is infinitely strong. The phase accumulated under the isotropic shift is given by

$$\tau = T - 2 \sum_{p=1}^q (-1)^{p-q} t^{(p)} \quad (10)$$

and when  $\tau = 0$  the end of the sequence coincides with a spin echo, so that phase shifts for different sites are avoided. For CSA amplification we set the required initial phase in Eq. (8) equal to the phase accumulated during the sequence of  $\pi$ -pulses in Eq. (9). Setting  $\tau = 0$  this gives

$$0 = (N - 1)\xi_c(0; \gamma) - N\xi_c(0; \gamma + \Xi) \\ + (-1)^q \left\{ 2 \sum_{p=1}^q (-1)^p \xi_c(t^{(p)} - T; \gamma) + \xi_c(-T; \gamma) \right\}. \quad (11)$$

For simplicity we assume here that  $T$  is an integer number of rotor periods and that  $q$  is odd. In this situation Eq. (11) becomes

$$0 = (N - 2)\xi_c(0; \gamma) - N\xi_c(0; \gamma + \Xi) - \left\{ 2 \sum_{p=1}^q (-1)^p \xi_c(t^{(p)}; \gamma) \right\}. \quad (12)$$

Using the definition and symmetry of  $\xi_c$ , Eq. (12) can be expanded to give

$$0 = N - 2 - N \exp(im\Xi) - \left\{ 2 \sum_{p=1}^q (-1)^p \exp(im\omega_r t^{(p)}) \right\} \quad (13)$$

for  $m = \pm 1$  and  $m = \pm 2$ . The form of Eq. (13) suggests that high amplification factors  $N$  can be obtained by constraining  $\pi$ -pulses with  $p$  even to coincide with a rotor echo. Setting  $q = N - 1$  results in timings for  $\pi$ -pulses of the form

$$t^{(p)} = \begin{cases} (k^{(p)} - \frac{\Xi}{2\pi}) \tau_r & p \in \text{odd} \\ k^{(p)} \tau_r & p \in \text{even} \end{cases}, \quad (14)$$

where  $k^{(p)}$  is an integer. This means that pulses with  $p$  even remain fixed on a rotor echo, while pulses with  $p$  odd are displaced to earlier times in a linear fashion with increasing



$$\varphi_j = -\frac{2\pi qj}{2q+1}, \quad (16)$$

where  $j$  is the scan counter, while all  $\pi$ -pulses with  $p$  even, as well as the contact pulse, are cycled according to

$$\varphi_j = -\frac{2\pi(q+1)j}{2q+1}. \quad (17)$$

Combination with a conventional phase alternation of the initial proton  $\pi/2$ -pulse concurrently with the receiver results in a manageable  $2(2q+1)$ -step overall phase cycle. Phase cycles and sample pulse programs for the  $q=15$  experiment are available on the Website <http://www.nottingham.ac.uk/~pczjt/>.

#### 4. Results and discussion

As an illustration of the method Fig. 2A shows the carbon-13 CSA amplification spectrum of  $\alpha$ -D-glucose (Aldrich) recorded at a Larmor frequency of 75.47 MHz and a MAS rate of 8 kHz. The amplification factor was 16, resulting in an effective MAS rate of 500 Hz. The 8 FIDs corresponding to the 8 required values of  $\mathcal{E}$  were obtained using the  $\pi$ -pulse timings of Eqs. (14) and (15). Other experimental parameters are given in the figure caption. The sideband intensities extracted from the  $\omega_1$  dimension of the spectrum (symbols) are compared with those obtained from the original CSA amplification experiment using a MAS rate of 4 kHz and an amplification factor of 8 (lines) in Fig. 2B. It should be noted that the relatively small carbon-13 shift anisotropies and the long spin–lattice relaxation times make carbohydrate molecules, such as glu-

cose, challenging examples. The good agreement between the sideband intensities demonstrates that the improved CSA amplification experiment functions correctly. The principal components of the shift tensors of  $\alpha$ -D-glucose measured from the improved CSA amplification experiment are given in Table 1. The difference between these values and those obtained using the original CSA amplification method was always less than 2 ppm.

As a further demonstration, Fig. 3 shows the aliphatic part of a carbon-13 CSA amplification spectrum of L-methionine (98%, Aldrich), recorded at a Larmor frequency of 75.47 MHz and a MAS rate of 8 kHz. The amplification factor was 32, resulting in an effective MAS rate of 250 Hz. Other experimental parameters are given in the figure caption. Most of the resonances in the spectrum are split into two components, suggesting the presence of two polymorphs, as observed previously [1].

The theory of CSA amplification described above assumes  $\pi$ -pulses which are infinitesimally short, exactly

Table 1  
CSA amplification measurements of principal components of shift tensors in  $\alpha$ -D-glucose

Site <sup>a</sup>	$\sigma_{11}$ (ppm) <sup>b</sup>	$\sigma_{22}$ (ppm)	$\sigma_{33}$ (ppm)
1	72.9	87.8	117.4
2	90.4	72.9	48.0
3	90.7	72.9	55.1
4	55.7	70.0	91.8
5	93.7	71.5	49.3
6	87.6	68.0	35.2

<sup>a</sup> Sites are labeled according to the IUPAC convention.

<sup>b</sup> Labeled according to  $|\sigma_{22} - \sigma_{\text{iso}}| < |\sigma_{11} - \sigma_{\text{iso}}| < |\sigma_{33} - \sigma_{\text{iso}}|$ .

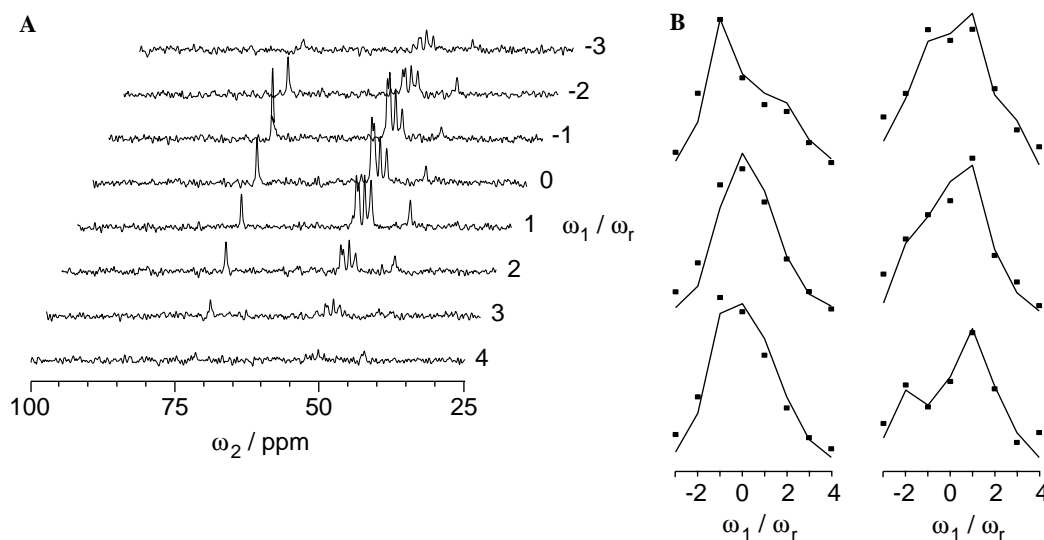


Fig. 2. (A) Carbon-13 CSA amplification spectrum of  $\alpha$ -D-glucose recorded at a Larmor frequency of 75.47 MHz and a MAS rate of 8 kHz. The amplification factor was 16, resulting in an effective MAS rate of 500 Hz. The MAS rate was stabilized to  $\pm 5$  Hz, and the contact time was 2.5 ms. The proton decoupling field was approximately 85 kHz, and carbon-13  $\pi$ -pulses were 4.8  $\mu$ s in duration. The spectral width in  $\omega_2$  was 27.3 kHz and the acquisition time was 75.1 ms. The relaxation delay was 50 s, and there were 124 scans for each of the 8 sequences required. (B) Sideband intensities extracted from the spectrum (points) in (A), compared with those extracted from the original CSA amplification (lines) experiment using a MAS rate of 4 kHz and an amplification factor of 8. Left-hand column from the top: carbon sites 1, 3, and 4, right-hand column from the top: carbon sites 5, 2, and 6, according to the IUPAC convention.

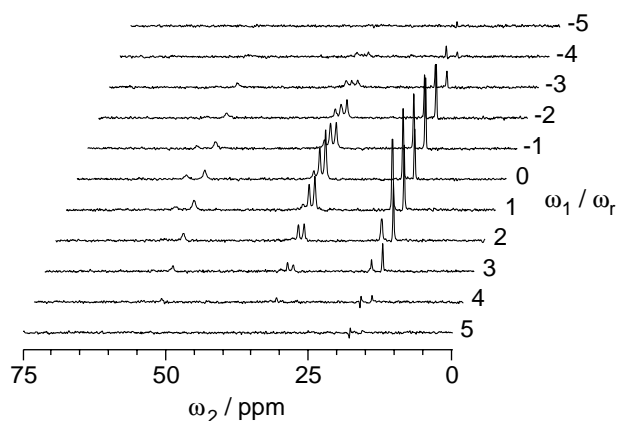


Fig. 3. Aliphatic part of the carbon-13 CSA amplification spectrum of L-methionine recorded at a Larmor frequency of 75.47 MHz and a MAS rate of 8 kHz. The amplification factor was 32, resulting in an effective MAS rate of 250 Hz. The MAS rate was stabilized to  $\pm 5$  Hz, and the contact time was 1 ms. The proton decoupling field was approximately 85 kHz, and carbon-13  $\pi$ -pulses were 5.0  $\mu$ s in duration. The full spectral width in  $\omega_2$  was 27.3 kHz and the acquisition time was 75 ms. The relaxation delay was 6 s, and there were 504 scans for each of the 16 sequences.

synchronized with the MAS rotor and correctly calibrated. In practice, experimental imperfections, such as fluctuations in the MAS rate and  $B_1$  inhomogeneity, as well as off-resonance effects are expected to cause distortions of the sideband intensities. In order to investigate this further, simulations have been carried out using the SIMPSON program due to Bak et al. [13]. The simulations shown here involve a carbon-13 nucleus with a chemical shift anisotropy (defined as  $\delta = \sigma_{33} - \sigma_{iso}$ ) of 25 ppm and an asymmetry (defined as  $\eta = (\sigma_{22} - \sigma_{11})/\delta$ ) of 0.25. In each case the Larmor frequency was 75.47 MHz and the MAS rate was 16 kHz. CSA amplification by a factor 16 was achieved with  $q = 15$ , giving an apparent rate of 1 kHz in the  $\omega_1$  dimension. The two-dimensional spectrum which results from this sequence with 8 values of  $\Xi$  was generated by direct calculation of the full MAS propagator for the entire pulse sequence, including the effect of finite rf amplitude. Powder averaging was achieved using 66 ( $\alpha, \beta$ ) orientations, following the REPULSION scheme [14] and 40 uniformly distributed  $\gamma$  values. The rf amplitude was 60 kHz in all cases. The mismatch between the sideband intensities simulated for CSA amplification and those expected from MAS was quantified using the parameter [3]

$$\chi^2 = \sum_j (I_j - I_j^{MAS})^2. \quad (18)$$

In our experience for the parameters used here a  $\chi^2$  value above 0.5 results in an unacceptable error of more than 2 ppm in the principal components of the measured shift tensors.

Fig. 4 summarizes the results of the simulations. In Fig. 4A the actual MAS rate deviated from the nominal rate of 16 kHz by up to  $\pm 100$  Hz. The resulting variation

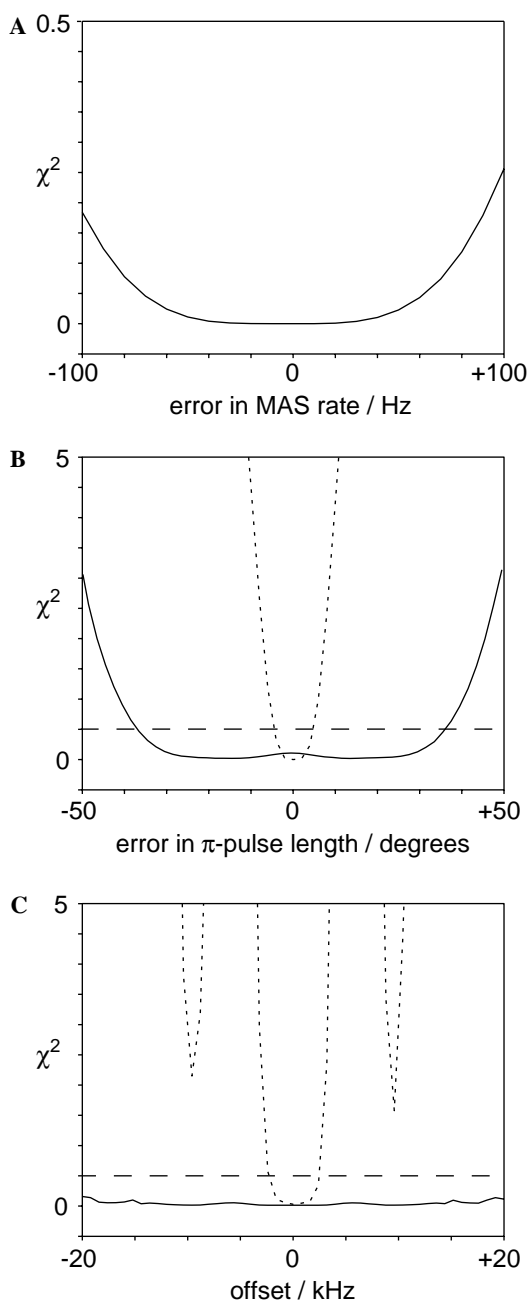


Fig. 4. Simulations which illustrate the effect on the reliability of the CSA amplification experiment of fluctuations in the MAS rate. The plots show the mismatch parameter  $\chi^2$  as a function of (A) the actual MAS rate, (B) the  $\pi$ -pulse length and (C) the offset for simulated CSA amplification experiments as described in the text. In (B and C) the solid line explicitly includes COGWHEEL phase cycling, while the dots do not. The dashes represent the level below which the mismatch parameter becomes unacceptable.

of the mismatch parameter  $\chi^2$  indicates that the improved CSA amplification experiment is very robust with respect to fluctuations in the MAS rate. Provided that the MAS rate can be stabilized to within  $\pm 30$  Hz, the mismatch between the CSA amplification sideband pattern and that expected for MAS is insignificant. Even if the actual MAS rate deviates from the nominal rate by  $\pm 100$  Hz,

the mismatch parameter remains within the acceptable range.

In Fig. 4B the effect of pulse length miscalibration and  $B_1$  inhomogeneity is illustrated. Two sets of simulations were carried out in which the flip angle of the  $\pi$ -pulses deviated from  $180^\circ$  by up to  $\pm 50^\circ$ . For the first set (dots) the phases of all  $\pi$ -pulses remained constant, while for the second set (solid line) they were phase cycled according to the COGWHEEL procedure described above, and the results co-added and normalized. The dashes indicate the level below which the mismatch parameter remains acceptable. The resulting plots indicate that without the COGWHEEL phase cycle a miscalibration of less than  $\pm 5^\circ$  is sufficient to completely frustrate the correct operation of the experiment. Given the  $B_1$  inhomogeneity of commercial MAS probes, this degree of accuracy in calibration is not achievable for the whole sample without substantially restricting its volume. However, the COGWHEEL phase cycle largely eliminates this problem, making the experiment practicable. In this case miscalibration of up to  $\pm 30^\circ$  does not affect the reliability of CSA amplification, although in practice the resulting degradation in signal-to-noise may render analysis of the sidebands impossible.

Finally, Fig. 4C shows the effect of resonance offset which was varied across a range of  $\pm 20$  kHz. Once again sets of simulations were carried out with (solid line) and without (dots) the COGWHEEL phase cycle. The resulting plots indicate that the COGWHEEL phase cycle is mandatory if a spectral dispersion of more than  $\pm 2$  kHz is present. In all cases the detailed shape of the plots varies with the CSA tensor and experimental factors, such as MAS rate and rf amplitude, but the overall conclusions about reliability remain unchanged.

## 5. Conclusions

The main advantage of the CSA amplification experiment [1,3] is that evolution under the isotropic part of the chemical shift is restricted to the detection dimension, such that long two-dimensional experiments can be avoided. In the improved version described here sensitivity is maximized by eliminating the need to store the magnetization along the  $z$ -axis for  $t_1$ . In addition, high amplification factors  $N$  can be obtained without resorting to the overly long sequences of  $\pi$ -pulses used in a recent modification [7]. Amplification factors as high as 32 have been demonstrated experimentally, and the principal components of the CSA tensor extracted from the resulting spectra have been shown to be reliable. The improved

experiment functions as a genuine alternative to 2D-PASS, since the duration of the sequences required in the two experiments are identical for the same effective MAS rate. However, CSA amplification has the advantage that slow MAS rates are not required to measure small shift anisotropies.

## Acknowledgments

This research was supported in its early stages by the EPSRC (Grants GR/L26742 and GR/N02023, as well as a studentship for CC). L.S. thanks Universities UK, for an ORS Scholarship.

## References

- [1] C. Crockford, H. Geen, J.J. Titman, Two-dimensional MAS NMR spectra which correlate fast and slow magic angle spinning sideband patterns, *Chem. Phys. Lett.* 344 (2001) 367.
- [2] C. Crockford, H. Geen, J.J. Titman, Measurement of orientation distributions using chemical shift amplification, *Solid State Nucl. Magn. Reson.* 22 (2002) 298.
- [3] L. Shao, C. Crockford, H. Geen, G. Grasso, J.J. Titman, Chemical shift anisotropy amplification, *J. Magn. Reson.* 167 (2004) 75.
- [4] S. Féaux de Lacroix, J.J. Titman, A. Hagemeyer, H.W. Spiess, Increased resolution in MAS NMR spectra by two-dimensional separation of sidebands by order, *J. Magn. Reson.* 97 (1992) 435.
- [5] O.N. Antzutkin, S.C. Shekar, M.H. Levitt, Two-dimensional sideband separation in magic angle spinning NMR, *J. Magn. Reson. A* 115 (1995) 7.
- [6] W.T. Dixon, Spinning-sideband-free and spinning-sideband-only NMR spectra in spinning samples, *J. Chem. Phys.* 77 (1982) 1800.
- [7] R.M. Orr, M.J. Duer, S.E. Ashbrook, Correlating fast and slow chemical shift spinning sideband patterns in solid-state NMR, *J. Magn. Reson.* 174 (2005) 301.
- [8] O.N. Antzutkin, Z. Song, X. Feng, M.H. Levitt, Suppression of sidebands in magic angle spinning nuclear magnetic resonance—general principles and analytical solutions, *J. Chem. Phys.* 100 (1994) 130.
- [9] H.W. Spiess, in: P. Diehl, E. Fluck, R. Kosfeld (Eds.), *NMR, Basic Principles and Progress*, Springer, Berlin, 1978.
- [10] O.N. Antzutkin, Sideband manipulation in magic angle spinning nuclear magnetic resonance, *Prog. Nucl. Magn. Reson. Spectrosc.* 35 (1999) 203.
- [11] M.H. Levitt, P.K. Madhu, C.E. Hughes, Cogwheel phase cycling, *J. Magn. Reson.* 155 (2002) 300.
- [12] N. Ivchenko, C.E. Hughes, M.H. Levitt, Application of cogwheel phase cycling to sideband manipulation experiments in solid-state NMR, *J. Magn. Reson.* 164 (2003) 286.
- [13] M. Bak, J.T. Rasmussen, N.C. Nielsen, SIMPSON: A general simulation program for solid-state NMR spectroscopy, *J. Magn. Reson.* 147 (2000) 296.
- [14] M. Bak, N.C. Nielsen, REPULSION, a novel approach to efficient powder averaging in solid-state NMR, *J. Magn. Reson.* 125 (1997) 132.